Physica Medica 113 (2023) 102658

Contents lists available at ScienceDirect

Physica Medica

journal homepage: www.elsevier.com/locate/ejmp

Radioguided surgery with β decay: A feasibility study in cervical cancer

Angela Collarino [a,1], Anita Florit [b], Nicolò Bizzarri [c], Valerio Lanni [a], Silvio Morganti [d], Marco De Summa [e], Giuseppe Vizzielli [c], Francesco Fanfani [c,f], Riccardo Mirabelli [d,g,*], Gabriella Ferrandina [c,f], Giovanni Scambia [c,f], Vittoria Rufini [a,b], Riccardo Faccini [d,h], Francesco Collamati [d]

[a] Nuclear Medicine Unit, Fondazione Policlinico Universitario A. Gemelli IRCCS, Rome, Italy
[b] Section of Nuclear Medicine, University Department of Radiological Sciences and Hematology, Università Cattolica del Sacro Cuore, Rome, Italy
[c] Gynecologic Oncology Unit, Department of Women, Children and Public Health Sciences, Fondazione Policlinico Universitario A. Gemelli IRCCS, Rome, Italy
[d] National Institute of Nuclear Physics (INFN), Section of Rome, Rome, Italy
[e] PET/CT Center, Fondazione Policlinico Universitario A. Gemelli IRCCS, Rome, Italy
[f] Institute of Obstetrics and Gynecology, Università Cattolica del Sacro Cuore, Rome, Italy
[g] Department of Basic and Applied Sciences for Engineering, Sapienza Università di Roma, Rome, Italy
[h] Physics Department, Sapienza Università di Roma, Rome, Italy

ARTICLE INFO

Keywords:
β probe
Radioguided surgery
Cervical cancer
Monte Carlo simulation

ABSTRACT

Purpose: Radioguided surgery (RGS) is a technique that helps the surgeon to achieve a tumour resection as complete as possible, by means of the intraoperative detection of particles emitted by a radiotracer that bounds to tumoural cells. This study aimed to investigate the applicability of β-RGS for tumour resection and margin assessment in cervical cancer patients preoperatively injected with [^{18}F]FDG, by means of Monte Carlo simulations.

Methods: Patients were retrospectively included if they had a recurrent or persistent cervical cancer, underwent preoperative PET/CT to exclude distant metastases and received radical surgery. All PET/CT images were analysed extracting tumour SUV_{max}, background SUV_{mean} and tumour-to-non-tumour ratio. These values were used to obtain the expected count rate in a realistic surgical scenario by means of a Monte Carlo simulation of the β probe, assuming the injection of 2 MBq/kg of [^{18}F]FDG 60 min before surgery.

Results: Thirty-eight patients were included. A measuring time of ~2–3 s is expected to be sufficient for discriminating the tumour from background in a given lesion, being this the time the probe has to be over the sample in order to be able to discriminate tumour from healthy tissue with a sensitivity of ~99% and a specificity of at least 95%.

Conclusion: This study presents the first step towards a possible application of our β-RGS technique in cervical cancer. Results suggest that this approach to β-RGS could help surgeons distinguish tumour margins from surrounding healthy tissue, even in a setting of high radiotracer background activity.

1. Introduction

Cervical cancer is one of the most common malignancies in women worldwide [1]. About 40% of patients with cervical tumour has locally advanced cervical cancer (LACC) at initial diagnosis [2]. Exclusive chemo-radiotherapy (CRT) (i.e., without surgery) is the standard treatment for LACC [3]. However, one third of patients will develop disease recurrence, usually within two years after CRT [4]. Pelvic exenteration is the curative treatment for recurrent or persistent cervical cancer that is confined to the central or lateral pelvis after radiation therapy [3,5]. Pelvic exenteration aims to remove the tumour and achieve negative surgical margins, which is the most important prognostic factor [6,7]. To date, intraoperative surgical margins are evaluated by histology examination, which can be performed intra-operatively with frozen sections. However, the frozen section procedure is time consuming (it might take up to 30–45 min) and can lead to false negative results.

* Corresponding author at: Department of Scienze di Base e Applicate per l'Ingegneria, Sapienza Università di Roma, Via Antonio Scarpa 14, 00161 Rome, Italy.
E-mail addresses: angela.collarino@policlinicogemelli.it (A. Collarino), riccardo.mirabelli@roma1.infn.it (R. Mirabelli).
[1] Nuclear Medicine Unit, Fondazione Policlinico Universitario A. Gemelli IRCCS. L.go A. Gemelli 8, 00168, Rome, Italy.

https://doi.org/10.1016/j.ejmp.2023.102658
Received 1 March 2023; Received in revised form 7 July 2023; Accepted 5 August 2023
Available online 19 August 2023

Moreover, if the surgeon cuts through the tumour, cancer cells might spread in the abdominal cavity. Therefore, an improved intraoperative detection of surgical margins could help to provide a more personalized treatment strategy.

In this view, radioguided surgery (RGS) could aid the surgeon in removing the tumour with negative margins. However, RGS with gamma (γ) decay is hardly applicable in this context. In fact, despite known 2-deoxy-2-[^{18}F]fluoro-D-glucose ([^{18}F]FDG) uptake of cervical tumour [8,9], the proximity of several organs (e.g., bladder, ureters) presenting elevated physiological [^{18}F]FDG uptake hinders the effective detection of residual tumour due to the long penetration of γ particles. An innovative approach to RGS has been recently introduced using a beta (β) probe with low sensitivity to γ radiation [10–14]. The rationale of this approach is that β radiation has lower penetration compared to γ radiation (few mm for *β versus* few/tens of cm for γ in human tissues). Being sensitive only to radiation coming from its immediate surroundings, a β probe could better discriminate the tumour margins (*signal*) from the nearby healthy tissue (*background*).

The idea of directly detecting β radiation is not new, and it was actually the very first approach to the RGS technique itself, back in 1949 [15]. More recently, other approaches to β-RGS were proposed [16], that however did not eventually result in any standard clinical practice, probably also due to the cumbersome design of these detectors, being based on the simultaneous detection of β and γ particles.

A more relevant development has been instead experienced by Cherenkov luminescence imaging [17–19], a technique based on the detection of Cherenkov radiation emitted by the target tissues after the injection of a PET radiotracer. Recent studies have also assessed the feasibility of evaluating surgical margins of specimens with intraoperative imaging performed with micro-PET/CT [20–22]. However, despite sharing the requirement for a β emitter, these techniques could be considered complementary to direct β radiation detection, since their current use is mainly focused on ex-vivo confirmation/margin assessment. In the last years, a new interest around β-RGS arose, thanks to the development of new scintillating materials allowing to build efficient β particle detectors [12] in convenient form factors, suitable for example for minimal invasive surgery.

To our knowledge, no previous studies have investigated this new technique for recurrent/persistent cervical cancer.

In this study, we aim to investigate the applicability of β-RGS for tumour resection with negative surgical margins in recurrent/persistent cervical cancer patients injected with [^{18}F]FDG, by means of Monte Carlo simulations based on [^{18}F]FDG uptake from preoperative PET/CT images.

2. Methods

2.1. Study design and patient population

This study was approved by the Ethical Committee of the Fondazione Policlinico Universitario A. Gemelli IRCCS (study code: 3859). The medical records of all consecutive patients with histologically proven cervical cancer, referred to the Gynecologic Oncology Unit between September 2013 and October 2020, were retrospectively reviewed. Patients were included if they signed an informed consent, had pelvic recurrent/persistent cervical cancer, underwent preoperative PET/CT to exclude distant metastases and received radical surgery (i.e., pelvic exenteration). Patients were excluded if they had contraindication for radical surgery due to age or comorbidities or extra-pelvic disease extension. All cases were discussed in a multidisciplinary board before undergoing radical surgery.

2.2. [^{18}F]FDG PET/CT image acquisition

PET/CT studies were acquired as previously described [23]. Briefly, each patient fasted for at least 6 h, had glucose blood levels <200 mg/dL before [^{18}F]FDG injection and was hydrated with 500 mL of saline solution. PET/CT imaging was acquired 60 ± 10 min post intravenous injection of [^{18}F]FDG using a Gemini GXL (Philips Healthcare, Best, The Netherlands) or a Biograph mCT (Siemens Healthineers, Erlangen, Germany) scanner. A low-dose CT scan was first performed for anatomical reference and attenuation correction followed by PET scan using 3 min (Gemini) and 2.5 min (Biograph mCT) acquisitions per bed position. All PET images were reconstructed according to the European Association of Nuclear Medicine guidelines [24], as described in Table 1. All PET/CT images were displayed on a dedicated workstation (Syngo. via Workstation, Siemens Healthineers, Erlangen, Germany) in transaxial, coronal and sagittal planes.

2.3. Image analysis

All PET/CT images were reviewed by consensus between two nuclear medicine physicians (A.F. and V.L., with 3 and 10 years of clinical experience, respectively), blinded to clinical and histopathological information.

A volume of interest (VOI) of 0.7–1.5 cm^3 was delineated over the tumour (T-VOI) and over the background tissue (B-VOI) on the transaxial PET images using a 3D-isocontour method based on a 40% threshold of the SUV_{max} corrected for local background activity (Fig. 1) [25,26]. The internal obturator muscle tissue was chosen as background tissue, as discussed later in the paper.

For each VOI, SUV_{max} was extracted for tumour (T-SUV_{max}) and SUV_{mean} for background (B-SUV_{mean}). SUV_{max} was measured by applying the EQ·PET reference-based quantification technology (Siemens Medical Solutions USA, Inc., Malvern, PA, USA) in order to harmonize SUV values obtained by 2 different PET systems [27]. The optimized spatial filters were selected as described by Mattoli et al. [28]: an 8-mm Gaussian filter was applied for the Biography mCT, while no EQ•PET Gaussian filter was needed for GXL system in order to align to EARL/EANM standards [24]. For evaluating uncertainties, root mean square SUV (SUV_{rms}) and VOI volumes (V_{Voi}, made of N_{Voxels}, number of voxels, with a V_{Voxel} volume) were also extracted, in order to calculate:

$$\sigma_{SUV} = \frac{SUV_{rms}}{\sqrt{N_{Voxels}}} = \frac{SUV_{rms}}{\sqrt{\frac{V_{Voi}}{V_{Voxel}}}}$$

i.e., the uncertainty on SUV. Tumour-to-non-tumour ratio (TNR) was defined as the ratio between the T-SUV_{max} and the B-SUV_{mean}.

Table 1
Specifications of PET/CT systems.

PET/CT scanner		Philips Gemini GXL	Siemens Biograph mCT
PET reconstruction protocol	Reconstruction	LOR-RAMLA (3 iterations, 33 subsets)	3D-OSEM with PSF modelling + TOF (2 iterations, 21 subsets)
	Gaussian filter (mm)	0	2.0
	Voxel size (mm^3)	4.0 × 4.0 × 4.0	3.2 × 3.2 × 5.0
	Slice thickness (mm)	4.0	5.0
	EQ•PET filter (mm)	0	8.0
CT protocol	Voltage (kV)	120	120
	Intensity (mAs)	40–50	40–50

LOR-RAMLA: Line-of-response row-action maximum likelihood algorithm. 3D-OSEM: 3-Dimensional ordered subsets expectation–maximization algorithm. PSF: Point spread function. TOF: time of flight.

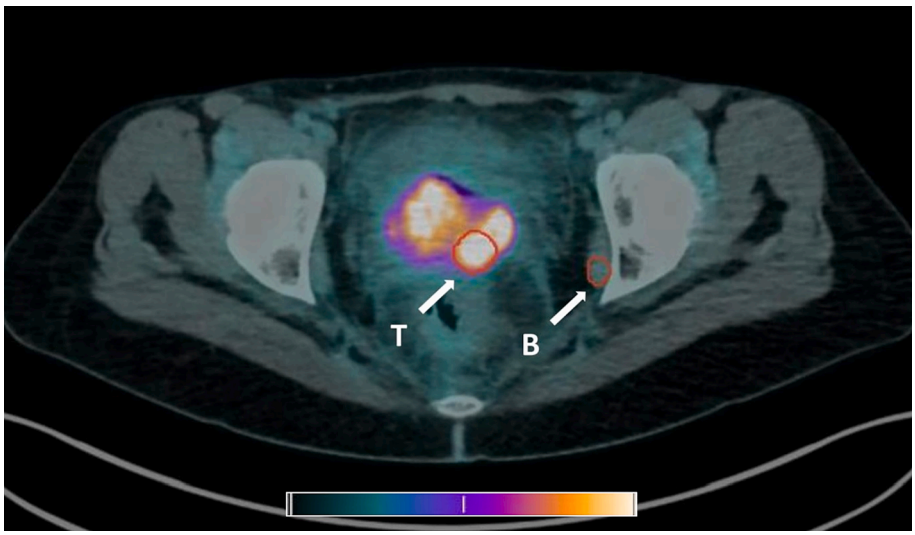

Fig. 1. Example of VOI identification in the tumour (T-SUV_{max} = 12.98) and in the background (B-SUV_{mean} = 1.21). SUV window limits: bottom = 0; top = 5.

2.4. β counting probe

The detector used in this study is composed of a cylindrical p-terphenyl scintillator (5-mm diameter and 3-mm height), encapsulated in a 12-mm diameter plastic ring lateral shielding, and covered in the front by a 15-μm aluminium foil for light tightness. Light collection was performed by a 3 × 3 mm^2 Silicon Photomultiplier sensor (SiPm, SensL C-series 30035).

Given the low energy β-decay and abundant flux of annihilation photons, a second version of the detector was also considered in this study, still having 5-mm diameter but with 2-mm height. The rationale is that this thickness of scintillator should already be enough to effectively absorb such low energy β particles, with a small reduction in charged-particle detection efficiency with respect to the 3-mm thick detector. At the same time, however, such a thinner detector allows for a marked reduction, for purely geometrical reasons, of the number of detected 511 keV photons. As a result, a 5 × 2 mm detector could be more efficient for [^{18}F]FDG, enhancing the β/γ detection ratio.

Bearing in mind a possible robotic surgery approach, in the Monte Carlo simulations on which this study was based, the β detector was placed at the tip of the DROP-IN probe housing [29], tailored to the ProGrasp Forceps (Intuitive Surgical Inc., Sunnyvale, CA, USA). Fig. 2A shows both the prototypes of the probe, either for open or robotic surgery.

2.5. Monte Carlo simulation of expected counting rates

Tumour and "near background". Once the uptake values of both tumour and background were obtained from the PET images, in order to quantify the performances of the technique, it was necessary to evaluate the counting rates that were expected in the two regions in a real application case. This procedure was the same used in previous similar studies [11,14], and relied on a Monte Carlo simulation in which the probe was exposed to (and in contact with) two different sources: a small tumoural remnant ("residual tumour") encapsulated in a healthy tissue cylinder ("near background"), and an area of sole healthy tissue. A diameter of 6 mm and a height of 7 mm were chosen for the tumour remnant (volume = 0.2 mL, Fig. 2B), while 2 cm diameter and 1 cm height were chosen for the healthy tissue sample (volume = 3.14 mL, Fig. 2C). As far as the tumour remnant is concerned, these dimensions are assumed to represent typical residual lesions that can be tailored in RGS procedures. This working hypothesis is at the basis of several similar studies that were performed in the past, and that found experimental validation both ex-vivo and in vivo [11,14]. On the other hand, since [^{18}F]FDG positrons, having a maximum energy of 630 keV, cannot penetrate more than 5 mm in human tissue, the chosen dimensions for the so-called "near background" sample are sufficient to reproduce all the physical processes that are the origin of this kind of contribution.

Both the "residual tumour" and the "near background" samples were

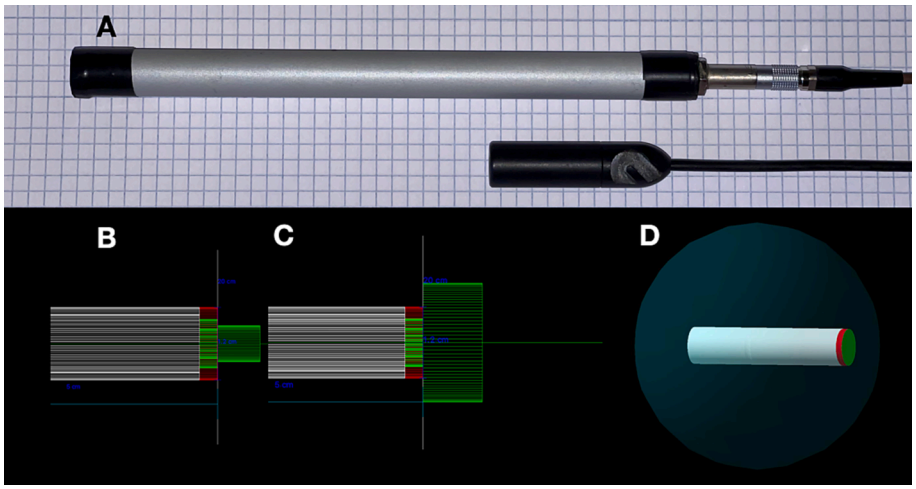

Fig. 2. β probe, in its "open surgery" (top) and "robotic surgery" (bottom) configurations (A), the foreground paper has 4-mm squares. Monte Carlo simulations used in this study: "residual tumour" (B); "near background" (C); in both cases, the right green cylinder represents the source, while the inner, green part of the probe is the p-terphenyl crystal, the rest being the lateral shielding. Beta probe inserted in the spherical VOI used for the "far background" simulation (D). (For interpretation of the references to colour in this figure legend, the reader is referred to the web version of this article.)

considered to have a specific activity (i.e., the activity per unit volume) according to that given by the SUV extracted from the PET analysis. In particular, the conversion between SUV and specific activity was performed assuming an injection of 2 MBq/kg (0.05 mCi/kg) of [^{18}F]FDG 60 min before surgery. A typical SUV of 10 would thus give a specific activity of 13.7 kBq/mL (0.37 μCi/mL).

"Far background". Given the known and abundant physiological uptake of [^{18}F]FDG in organs all around the pelvic region, a substantial flux of annihilation photons is expected to be present when performing rate measurements in the surgical field. Although the scintillator used in the β probe is largely transparent to annihilation photons, as noted, their contribution to the measured signal should nevertheless be evaluated.

To this aim, a dedicated and different Monte Carlo simulation was performed, based on a PET/CT image of a single reference patient, to evaluate the flux of annihilation photons reaching the pelvic area. In particular, PET images acquired after pelvic exenteration in a patient also studied pre-operatively were used, in order to best represent the application case, in which counting rate measurements would be performed after the removal of bladder and uterus, which are both organs characterized by elevated physiological uptake of [^{18}F]FDG. In this simulation, CT data were used to reconstruct the geometry of the patient, with all the relevant materials and their densities, while PET data were used to reproduce the distribution of [^{18}F]FDG (Fig. 3A). A spherical VOI (8 cm diameter) was drawn in the pelvic area (Fig. 3A), and the probe was placed at its centre (Fig. 2D). The number of simulated ^{18}F decays was chosen in order to reproduce the count rate that the probe would give in 1 s of data acquisition per each MBq of activity in the patient. In this way, by multiplying this value for the amount of [^{18}F]FDG present in the patient at the time of surgery, the expected probe counting rate at that exact time was obtained.

All simulations were performed using GEANT4 [30], a Monte Carlo code widely used in particle physics as well as in medical applications, that allows simulating all the relevant physical phenomena, like energy loss, particle propagation and secondary particles creation and interaction.

2.6. Statistical analysis

2.6.1. Minimal probing time

The two Monte Carlo simulations here described gave the following three count rates: R_{Tum}, the counting rate given by the residual itself, R_{HT}, the counting rate given by the healthy tissue nearby the tumour and R_{Far}, the counting rate coming from the annihilation photon flux and thus affecting all measurements in the pelvic area. These values were combined to obtain the actual rates the probe would experience when in contact with the tumour remnants and with the healthy tissue, respectively:

$$R_{Signal} = R_{Tum} + R_{Far}R_{Background} = R_{HT} + R_{Far}.$$

From these counting rate values, it was possible to estimate the minimal probing time (t_{probe}), i.e., the number of seconds (standard probe integration time) needed for the probe to be able to discriminate with sufficient accuracy the tumour from the healthy tissue.

To this aim, the same approach followed in other similar studies [11,14,31] was used, based on the estimation of the fraction of false positives (FP) and false negatives (FN) signals. In fact, for a given value of t_{probe}, the number of counts coming from signal and background is distributed according to a Poisson distribution having mean value $\mu_{Signal} = R_{Signal} \times t_{probe}$ and $\mu_{Background} = R_{Background} \times t_{probe}$, respectively. Given then a certain value for the minimum number of probe counts (th) considered as threshold to flag as positive a residual, FP was computed as the fraction of times the background would instead give a positive signal:

$$FP = 1 - \sum_{N=0}^{th-1} P_{\mu_{Background}}(N),$$

where $P_{\mu}(N)$ is the Poission probability to have N countings if the mean expected value is μ. Similarly, FN is the fraction of times a tumour residual would not give a positive signal:

$$FN = \sum_{N=0}^{th-1} P_{\mu_{Signal}}(N).$$

In order to determine the minimum probing time, t_{probe} and th were varied in a grid, and for each couple of values FN and FP were computed: the smallest value of t_{probe} for which $FN < 5\%$ and $FP \approx 1\%$ was determined, corresponding to a sensitivity of ~99% and a specificity of at least 95%.

2.7. ROC analysis

The described algorithm allows identifying the optimum probe counting time for each lesion. As a matter of fact, this parameter is not completely informative when dealing with a real application case, i.e., during the RGS procedure. In practice, however, in the course of

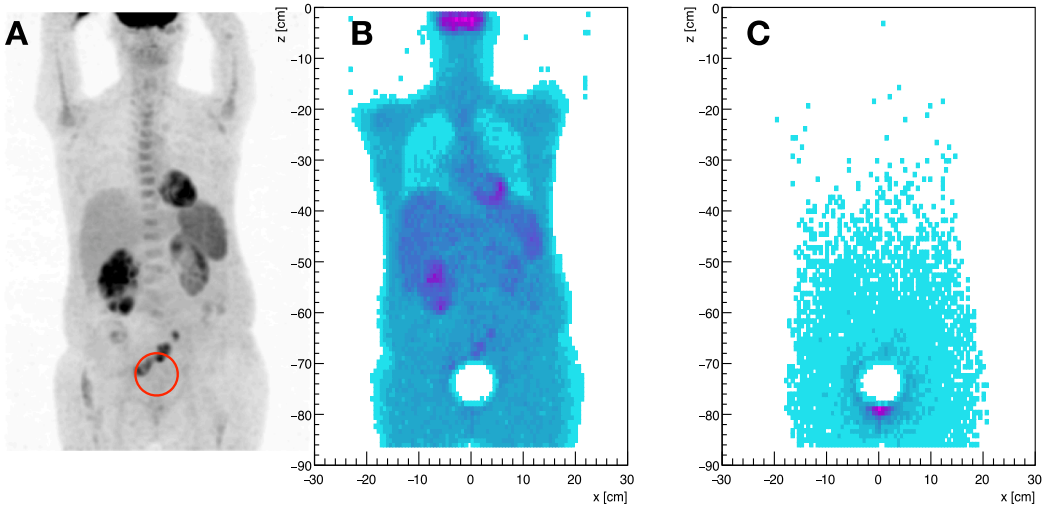

Fig. 3. Positioning in the pelvic area of the VOI needed for the "far background" Monte Carlo simulation, in a maximum intensity projection image of postoperative PET (A). Map (central slice) of primary particles generated in the Monte Carlo simulation, according to the PET image (B). Origin position of [^{18}F]FDG isotopes that eventually give a signal into the probe (C).

deciding whether malignant tissue is or is not present, surgeons tend to use a near-constant interval, of approximately 3 s in our experience of *ex-vivo* and *in-vivo* tests [32–34], for counting of each location in the surgical field.

A sensitivity analysis was therefore also performed, with the aim of evaluating the discriminating power of the technique. A fixed probing time of $t_{probe} = 3s$ was assumed, and the threshold value *th*, intended as the total number of counts obtained in this time interval, was varied. For each *th* value, "sensitivity" and "specificity" were evaluated and plotted in a ROC curve, the area of which was then used to evaluate the discriminating power of the technique.

To illustrate this process, let's imagine a case in which $R_{Background}$ is 100 counts per second (cps) and R_{Signal} is 200 cps. A probing time of $t_{probe} = 3$ s would give $\mu_{Background} = 300$ counts and $\mu_{Signal} = 600$ counts. In this analysis, the threshold is varied between these two values (300 and 600 counts) in homogeneous steps, and for each threshold value FP and FN probabilities are calculated, as explained in the text. Each of these steps corresponds to a point in the ROC curve, and the top left one allows estimating the intrinsic power of the procedure to distinguish healthy tissue from tumour.

3. Results

3.1. Patients

A total of 38 patients fulfilled the inclusion criteria and were included in this study. The median age at time of recurrent/persistent disease was 49.5 years (range, 32–74). Twenty-eight (73.7%) patients underwent exclusive radiochemotherapy, while the remaining ten (26.3%) had already undergone previous surgeries (e.g., radical hysterectomy), followed by radiotherapy or radiochemotherapy. Thirty-three (86.8%) women had the recurrence in the central pelvis, while 5 (13.2%) had lateral pelvis recurrent/persistent tumour. The administered activity of [^{18}F]FDG was 2.88–5.13 MBq/kg (Standard Deviation (SD), 0.70) (0.08–0.14 mCi/kg; SD, 0.02). PET/CT studies were acquired using Biograph mCT and Gemini GXL scanner in 23 and 15 patients, respectively. The median time between the PET/CT scan and the pelvic exenteration was 36.5 days (range, 4–121).

3.2. Tumour and background uptakes

Median T-SUV_{max} was 10.2 (Interquartile Range (IQR), 7.7–12.3) and median B-SUV_{mean} was 1.0 (IQR, 0.7–1.2), with an average uncertainty of 3.5% and 3.3%, respectively. Given all the other sources of uncertainty that will affect the final probe counting rate (i.e., dose calibration, probe positioning, patient alignment), the contribution of the SUV uncertainty to overall count-rate uncertainty was considered negligible and therefore not propagated in estimating the overall count-rate uncertainty. Median TNR was 10.6 (IQR, 7.5–14.0). Fig. 4A-B show distribution of SUVs (T-SUV_{max} and B-SUV_{mean}) and its errors, while Fig. 4C-D show the distribution of TNRs for all 38 patients, and the scatter plot of T-SUV_{max} *versus* TNR.

3.3. Sensitivity analysis

Fig. 5 shows an example of ROC curve for one patient, with each triangle representing a different threshold value used to evaluate sensitivity and specificity (with higher threshold values corresponding to bottom left points, thus implying high specificity but low sensitivity), and the distribution of AUC of the sensitivity of the two probes (5 × 3 and 5 × 2 mm) for all 38 patients. All cases except four presented an AUC of at least 0.95, meaning a remarkably high sensitivity, with AUC values above 0.75 in all cases.

3.4. Expected probe counting rates

Table 2 shows the efficiencies of the two considered probes, obtained with the described Monte Carlo simulations, to signal and far background, with their relative variation.

Fig. 6 shows the expected probe counting rates obtained with the Monte Carlo simulation. In particular, Fig. 6A shows the expected "far background" for the two considered probes (5 × 3 and 5 × 2 mm), i.e.,

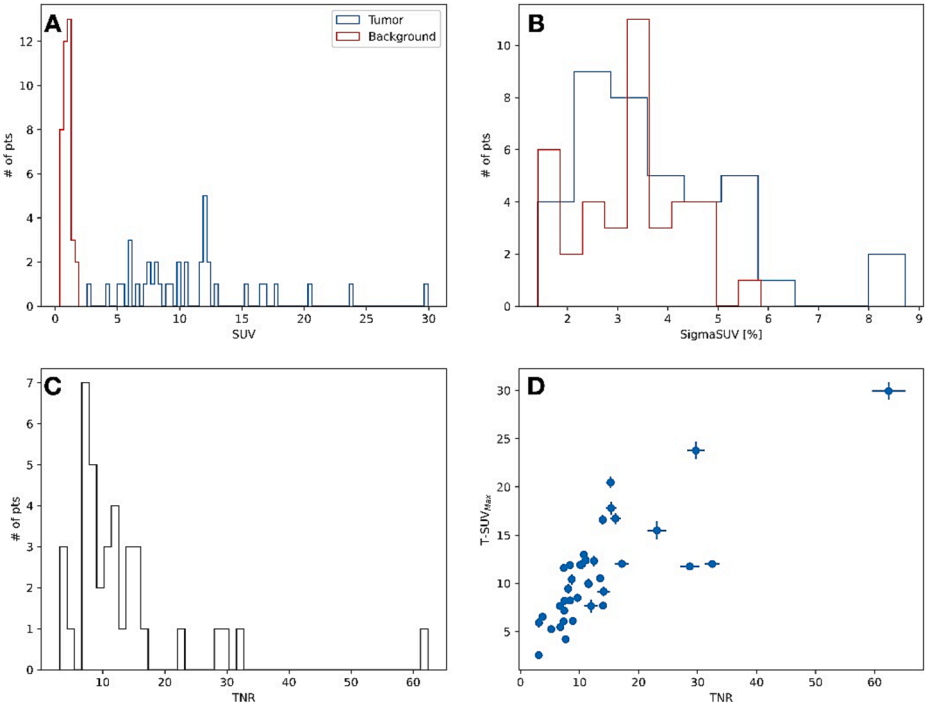

Fig. 4. Histograms of uptake of tumour (blue line) and background (red line). SUV (A). Histogram of error on SUV, calculated as described in the text, expressed in percentage of SUV value (B). Histogram of TNR (C). Scatter plot of T-SUV_{max} *versus* TNR (D). (For interpretation of the references to colour in this figure legend, the reader is referred to the web version of this article.)

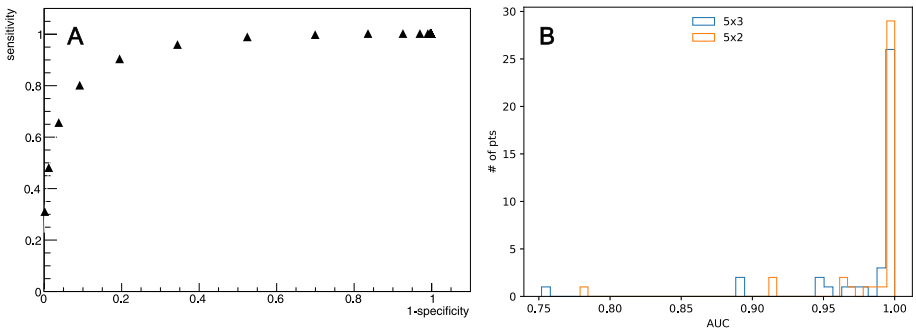

Fig. 5. Example of ROC curve for one patient (patient 6, sampling time 3 s, AUC value 0.94) (A). Distribution of AUC of the sensitivity analysis of the two probes (B).

Table 2
Efficiencies of the two probes, as obtained by the Monte Carlo simulations, to signal and far background, with their statistical uncertainties.

	5 × 3 mm probe	5 × 2 mm probe	Efficiency drop
Signal efficiency	(1.48 ± 0.01) 10^{-2}	(1.40 ± 0.01) 10^{-2}	−6%
Far background efficiency	(2.88 ± 0.17) 10^{-6}	(1.99 ± 0.14) 10^{-6}	−31%

the counting rate the probe would give as soon as it is inserted in the pelvic area, before being in contact with the suspect tumour lesion: a median counting value of 245 and 170 cps was found for the thicker and the thinner probe, respectively. The vast majority of this "far background" was indeed found to originate from the immediate surroundings of the pelvic area (Fig. 3C). In fact, despite having considered a post-exenteration sample patient, this area still remains dense of high emitting organs and tissues, whose emission has, for pure geometrical reasons, higher probability to be detected by the probe.

Fig. 6B and C, report scatter plots of R_{Signal} vs $R_{Background}$, for 5 × 3 and 5 × 2 probes, i.e., the counting rate expected when the probe is in contact with the tumour residual and the background respectively. The colour of each point corresponds to its AUC in the sensitivity analysis, with darker points having lower AUC.

3.5. Expected probe sampling time

The previously described procedure was used to obtain from the expected counting rates over signal and healthy tissue the minimum probing time, which is the time the probe has to be over the sample in order to be able to discriminate tumour from healthy tissue with a

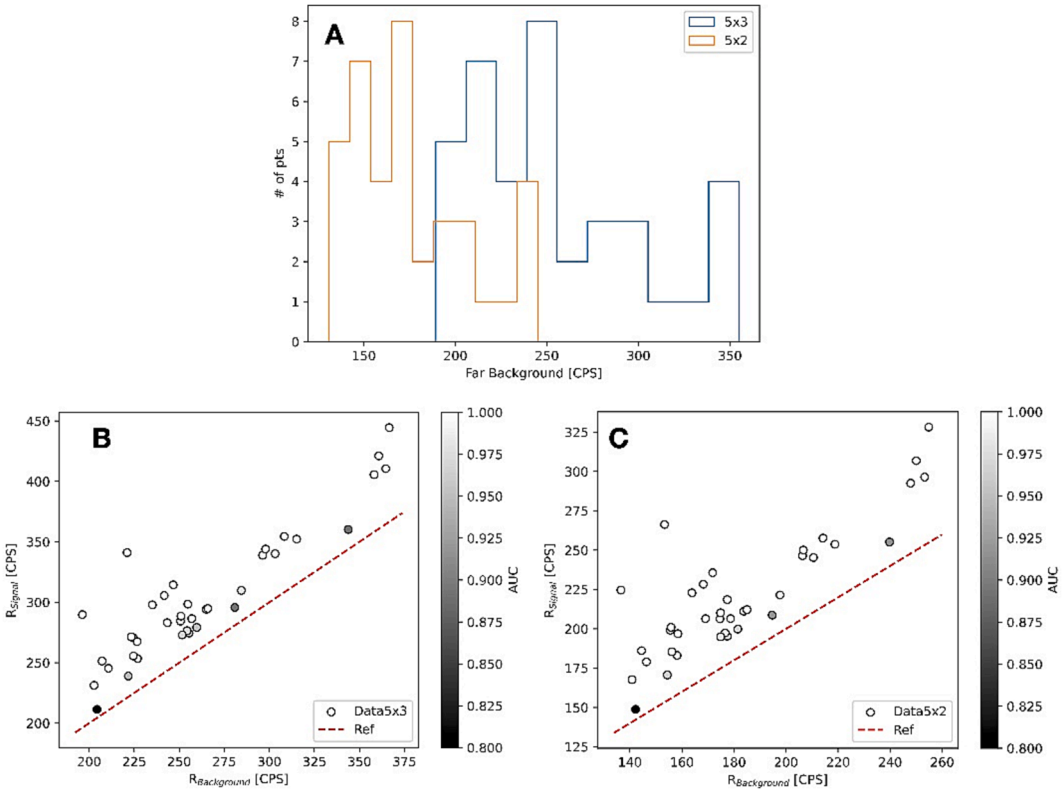

Fig. 6. Expected probe counting rates obtained with the Monte Carlo simulation. "Far background" for 5 × 3 mm and 5 × 2 mm probes (A). Scatter plot of R_{signal} vs $R_{background}$ for 5 × 3 mm (B) and 5 × 2 mm (C) probes respectively: the red dotted lines represent the bisector, i.e., the case in which the signal gives the same probe counting than the reference healthy tissue. Points' colour represents the corresponding AUC, according to the reported colour scale, with lighter points representing better results of the specificity-sensitivity analysis. (For interpretation of the references to colour in this figure legend, the reader is referred to the web version of this article.)

sensitivity of ~99% and a specificity of at least 95%. Fig. 7 shows the histogram (A) of this minimum probing time with the two probes. As highlighted by the relative box plot (B), median sampling time was found to be 2.48 (IQR, 1.86–2.95) and 2.37 (IQR, 1.57–3.94) for the 5 × 3 and 5 × 2 probes, respectively.

4. Discussion

This study evaluated the applicability of β-RGS in order to achieve negative surgical margins in recurrent/persistent cervical cancer after radiochemotherapy in patients injected with [^{18}F]FDG, by means of Monte Carlo simulations based on [^{18}F]FDG uptake from preoperative PET/CT images.

The β probe prototype used in the current study is based on a scintillating material (p-terphenyl) that is able to convert energy deposition from interacting particles into light. The detection of this light gives an estimation of the amount of radiation impinging on the crystal. The choice of p-terphenyl as scintillating material [35], characterized by a very abundant light production when traversed by radiation (the so called "light-yield"), ensures very high sensitivity to charged particles even in small active volumes. In particular, the effectiveness of cylindrical detectors as small as 3 mm in radius and 3 mm in depth was demonstrated in several studies using β^- emitters [32–34]. Moreover, the low density of p-terphenyl (1.24 g/cm^3) and relatively low effective atomic number, makes this material substantially insensitive to γ photons, whose interaction probability is higher in high density, high-Z materials. This intrinsic transparency to photons suggested to investigate a potential role of such detectors in performing RGS using β^+ emitting isotopes, where the contribution of annihilation photons becomes fundamental. Results of laboratory studies performed on ^{68}Ga source led to improve the probe (i.e., increasing the light collection efficiency), and to assess its efficiency to charged particles (which ranges from 80% at 110 keV to a plateau of 95% at higher energies, with the efficiency to γ photons being of the order of 3%) [36]. More recently, we conducted similar laboratory studies directly on ^{18}F liquid source. Recently published results [37], confirm the capability of the Monte Carlo simulation to accurately characterize the actual performances of the probe. Furthermore, the feasibility of RGS based on PET isotopes was also studied, starting with prostate cancer with [^{68}Ga]Ga-prostate-specific membrane antigen (PSMA) in robotic surgery [29]. *Ex-vivo* tests were then performed in this particular case, further strengthening the possibility of this novel approach [11,29]. Following these positive results, first *in-vivo* tests of RGS with our β probe are currently ongoing in case of abdominal neuroendocrine tumours and prostate cancer, using [^{68}Ga]Ga-PSMA as tracer, with very promising results.

In an effort to expand the use of this technique towards further application cases, in this study we present the first step of such a process, i.e., the Monte Carlo evaluation of the technique feasibility in case of recurrent/persistent cervical cancer after radiochemotherapy in patients injected with [^{18}F]FDG.

To this aim, preoperative PET/CT images of 38 patients were used to extract the [^{18}F]FDG uptake in both tumour and background. The SUV maximum value (SUV_{max}) was chosen for tumour, whereas its mean value (SUV_{mean}) was considered for the healthy background. This choice reflects the expected measurement procedure, as for example described in El Lakis et al. [38], in which the probe is used to find the maximum counting rate in a suspect lesion. This rate is then compared with the background one that, having by definition no specific and particular uptake, is averaged over a given area. As expected, a significant variation was found among patient T-SUV_{max} (range, 2.6–29.9). However, this variation occurs around a high median value (10.2), thus confirming high [^{18}F]FDG uptake of cervical tumour [8,9].

In this context, aiming at evaluating the maximum uptake of tumours, small VOIs were used, not needing to completely segment lesions.

As far as the background tissue choice is concerned, a possibility could have been represented by fatty tissue, since this is the one against which the surgeon is often expected to discriminate the tumour. However, the internal obturator muscle was eventually chosen because its specific activity is expected to be higher than the one of fatty tissue. In this way, we aimed to avoid a possible underestimation of the healthy tissue uptake. Other high activity regions are also expected to be present in the vicinity; however, due to the discussed short penetration of β radiation, the contribution of all sources not directly in contact with the probe is taken into account in the "far background" simulation. We found that "near background" presents a much smaller, albeit not negligible, [^{18}F]FDG uptake, not exceeding a $SUV_{mean} = 1.9$. As a result, TNR was high (median 10.6), with 90% of patients having TNR > 6.

Based on these [^{18}F]FDG uptake values, a Monte Carlo simulation was used to evaluate the expected counting rates of the probe in the surgical field, assuming an injected activity of 2 MBq/kg (0.05 mCi/kg) of [^{18}F]FDG 60 min before surgery. This simulation also considers the "far background", that is the number of annihilation photons in the surgical field (pelvic area) due to the unavoidable and physiological uptake of [^{18}F]FDG in the whole body. Indeed, we found this "far background" to be of the order of several hundreds of cps. This is, however, one of the cases in which the possible advantage of choosing a thinner detector arises. In particular, due to purely geometrical reasons, as demonstrated by probe efficiencies in Tab. 2, the 5 × 2 mm probe reduced the "far background" of the order of 100 cps compared to 5 × 3 mm probe, and could therefore represent a more suitable detector for this kind of application.

Considering all these aspects, the Monte Carlo simulation showed that the final probe counting in a real application case is expected to be of the order of several hundreds of cps. A statistical analysis on false positive and false negative probability evaluated the minimum required probing time to obtain a sensitivity of ~99% and a specificity of at least 95% to be of the order of ~2–3 s. This sampling time has a minimum

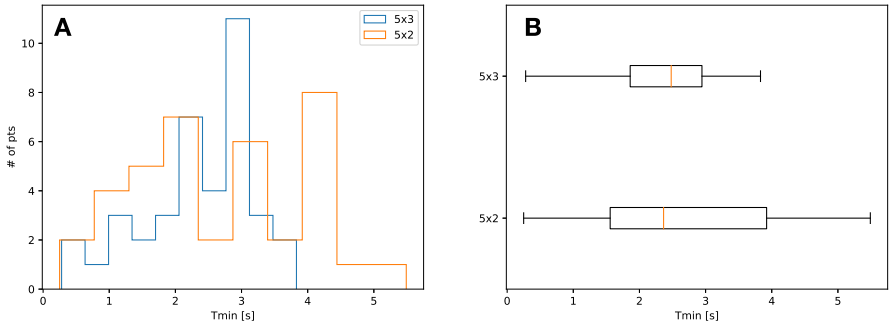

Fig. 7. Minimum probing time needed to effectively discriminate tumour from healthy tissue with the two considered probes (A), with respective box plots (B), in which the vertical, almost central line represents the median value, the box margins are the 25–75 percentiles, and the edges are Q1 ± 1.5 IQR.

effect on the whole surgery duration, considering that the surgeon is expected to spend this time only over spots judged suspect and needed to be discriminated. Moreover, the overall surgery time could be further reduced by avoiding the frozen section procedure.

Overall, results suggest that, with a probing time of 3 s, compatible with the standard clinical procedure, the β probe should have both a high sensitivity to β radiation and reduced sensitivity to 511 keV γ background to allow an effective performing of β-based RGS in recurrent/persistent cervical cancer. This innovative β probe may have important clinical applications. The potential use of this probe during pelvic exenteration would allow the surgeon to confirm in real time free surgical margins, with consequent reduction of operative time in a single session compared to the approach with frozen section analysis. Moreover, this probe is completely compatible with a robotic surgery scenario.

To our knowledge, this is the first study evaluating the applicability of β-RGS in cervical cancer using β probes. Nevertheless, this study suffered from some limitations. First and foremost, this study is mainly based on Monte Carlo simulations. However, it would probably be incorrect to define it as "simulation only". In fact, real clinical data play a significant role as input to the study. Moreover, the Monte Carlo simulation used in this study is being currently and steadily validated by the discussed *in-vivo* experimentations, which were based in turn on similar simulation studies in the first place. In a similar way, while it is clear that a study of this kind can only draw conclusions on statistical basis, the ongoing experimentations are also confirming the expectations regarding the "operative discriminating power" of the technique too, when the surgeon has to deal with given ratios of signal to background. Lastly, it is important to remember that these kinds of Monte Carlo studies are the necessary and sole possible first step towards any possible new experimental application of the β -RGS technique.

As far as other limitations of the study are concerned, this was a retrospective, single-centre study. Moreover, PET images were acquired on 2 different scanners and this could have minimally affected the SUV homogeneity [24,39]; however, EQ•PET was applied to harmonize SUV values. Lastly, the "far background" counting rate was only obtained by simulation, thus, its uncertainty and variability should be carefully considered. In particular, the count rate changes that may occur when performing small movements of the probe in the surgical field should be verified.

In this context, again, the first *in-vivo* measurements with [^{68}Ga]Ga-PSMA, currently in publication, represent a strong confirmation of the accuracy of our Monte Carlo simulations. In any case, results of this study seem solid enough that even significant variations and variability of the "far background" should not hinder the applicability of the technique, if properly dealt with. Besides the discussed possible use of a thinner probe to reduce the impact of this "far background", it could for example also be possible to act on the detector threshold in order to optimize the signal-to-noise ratio, foreseeing a "low background" operational modality for the probe.

As far as radio protection issues are concerned, the same considerations of previous β^+ radioguided surgery studies hold [40]. The exposure impact on the patient is comparable with a PET scan, the main issue being the exposure of medical staff. It has however to be noted that the considered application scenario is based on an injection that is performed 60 min before surgery: this can help to limit the impact on medical personnel not directly involved in surgery. Moreover, robotic surgery would allow to reduce the amount of dose given to the surgeon, who would be performing the procedure without being in close contact with the patient. Lastly, an experimental validation of the probe performances foreseen by this Monte Carlo study would open the way to a reduction in the amount of radioactivity to be injected. In fact, exploiting the demonstrated ability to use PET images to foresee the probe counting, it will be possible to tailor the amount of [^{18}F]FDG to inject the patient, based on its real tumour and background uptake.

5. Conclusion

This study showed that an innovative β-radioguided surgery technique has the potential to help the surgeon to distinguish tumour from surrounding healthy tissue in patients with recurrent/ persistent cervical cancer undergoing radical surgery, by injecting 2 MBq/Kg (0.05 mCi/kg) [^{18}F]FDG before surgery and with an estimated measuring time of 2–3 s per each suspect area. Further studies are needed to evaluate and *in-vivo* confirm the actual performances of the β probe.

Funding

The authors declare that no funds, grants, or other support were received during the preparation of this manuscript.

Declaration of Competing Interest

The authors declare that they have no known competing financial interests or personal relationships that could have appeared to influence the work reported in this paper.

References

[1] Sung H, Ferlay J, Siegel RL, Laversanne M, Soerjomataram I, Jemal A, et al. Global cancer statistics 2020: GLOBOCAN estimates of incidence and mortality worldwide for 36 cancers in 185 countries. CA Cancer J Clin 2021;71(3):209–49.
[2] Patel DA, Barnholtz-Sloan JS, Patel MK, Malone JM, Chuba PJ, Schwartz K. A population-based study of racial and ethnic differences in survival among women with invasive cervical cancer: analysis of surveillance, epidemiology, and end results data. Gynecol Oncol 2005;97(2):550–8. https://doi.org/10.1016/j.ygyno.2005.01.045.
[3] Cibula D, Pötter R, Planchamp F, Avall-Lundqvist E, Fischerova D, Haie Meder C, et al. The European society of gynaecological oncology/european society for radiotherapy and oncology/European society of pathology guidelines for the management of patients with cervical cancer. Int J Gynecol Cancer 2018;28(4):641–55. https://doi.org/10.1097/IGC.0000000000001216.
[4] Espenel S, Garcia M-A, Trone J-C, Guillaume E, Harris A, Rehailia-Blanchard A, et al. From IB2 to IIIB locally advanced cervical cancers: report of a ten-year experience. Radiat Oncol 2018;13(1). https://doi.org/10.1186/s13014-018-0963-8.
[5] Abu-Rustum NR, Yashar CM, Arend R, Barber E, Bradley K, Brooks R. NCCN Clinical Practice Guidelines in Oncology (NCCN guidelines). Cervical Cancer: Version 2023;1:2023.
[6] Chiantera V, Rossi M, De Iaco P, Koehler C, Marnitz S, Ferrandina G, et al. Survival after curative pelvic exenteration for primary or recurrent cervical cancer: a retrospective multicentric study of 167 patients. Int J Gynecol Cancer 2014;24(5):916–22. https://doi.org/10.1097/IGC.0b013e3182a80aec.
[7] Sardain H, Lavoue V, Redpath M, Bertheuil N, Foucher F, Levêque J. Curative pelvic exenteration for recurrent cervical carcinoma in the era of concurrent chemotherapy and radiation therapy. A systematic review. Eur J Surg Oncol 2015;41:975–85. https://doi.org/10.1016/j.ejso.2015.03.235.
[8] Kumar R, Dadparvar S. 18F-fluoro-2-deoxy-D-glucose-positron emission tomography (PET)/PET-computed tomography in carcinoma of the cervix. Cancer 2007;110:1650–3. https://doi.org/10.1002/cncr.22968.
[9] Kidd EA, Spencer CR, Huettner PC, Siegel BA, Dehdashti F, Rader JS, et al. Cervical cancer histology and tumor differentiation affect 18F-fluorodeoxyglucose uptake. Cancer 2009;115(15):3548–54. https://doi.org/10.1002/cncr.24400.
[10] Solfaroli Camillocci E, Schiariti M, Bocci V, Carollo A, Chiodi G, Colandrea M, et al. First ex vivo validation of a radioguided surgery technique with β-radiation. Phys Med 2016;32:1139–44. https://doi.org/10.1016/j.ejmp.2016.08.018.
[11] Collamati F, Bocci V, Castellucci P, De Simoni M, Fanti S, Faccini R, et al. Radioguided surgery with β radiation: a novel application with Ga68. Sci Rep 2018;8(1). https://doi.org/10.1038/s41598-018-34626-x.
[12] Camillocci ES, Baroni G, Bellini F, Bocci V, Collamati F, Cremonesi M, et al. A novel radioguided surgery technique exploiting β- decays. Sci Rep 2014;4(1). https://doi.org/10.1038/srep04401.
[13] Collamati F, Pepe A, Bellini F, Bocci V, Chiodi G, Cremonesi M, et al. Toward radioguided surgery with β- Decays: Uptake of a somatostatin analogue, DOTATOC, in meningioma and high-grade glioma. J Nucl Med 2015;56(1):3–8. https://doi.org/10.2967/jnumed.114.145995.
[14] Mancini-Terracciano C, Donnarumma R, Bencivenga G, Bocci V, Cartoni A, Collamati F, et al. Feasibility of beta-particle radioguided surgery for a variety of "nuclear medicine" radionuclides. Phys Med 2017;43:127–33. https://doi.org/10.1016/j.ejmp.2017.10.012.
[15] Selverstone B, Solomon AK, Sweet WH. Location of brain tumors by means of radioactive phosphorus. J Am Med Assoc 1949;140:277. https://doi.org/10.1001/jama.1949.02900380017004.
[16] Daghighian F, Mazziotta JC, Hoffman EJ, Shenderov P, Eshaghian B, Siegel S, et al. Intraoperative beta probe: a device for detecting tissue labeled with positron or

electron emitting isotopes during surgery. Med Phys 1994;21(1):153–7. https://doi.org/10.1118/1.597240.
[17] Spinelli AE, Boschi F. Novel biomedical applications of Cerenkov radiation and radioluminescence imaging. Phys Med 2015;31:120–9. https://doi.org/10.1016/j.ejmp.2014.12.003.
[18] Das S, Thorek DLJ, Grimm J. Cerenkov imaging. Adv Cancer Res 2014;124:213–34. https://doi.org/10.1016/B978-0-12-411638-2.00006-9.
[19] Ciarrocchi E, Belcari N. Cerenkov luminescence imaging: physics principles and potential applications in biomedical sciences. EJNMMI Phys 2017;4:14. https://doi.org/10.1186/s40658-017-0181-8.
[20] Göker M, Marcinkowski R, Van Bockstal M, Keereman V, Van Holen R, Van Dorpe J, et al. 18F-FDG micro-PET/CT for intra-operative margin assessment during breast-conserving surgery. Acta Chir Belg 2020;120(5):366–74. https://doi.org/10.1080/00015458.2020.1774163.
[21] Debacker JM, Schelfhout V, Brochez L, Creytens D, D'Asseler Y, Deron P, et al. High-resolution 18F-FDG PET/CT for assessing three-dimensional intraoperative margins status in malignancies of the head and neck, a proof-of-concept. J Clin Med 2021;10(16):3737.
[22] Debacker JM, Maris L, Cordier F, Creytens D, Deron P, Descamps B, et al. Direct co-registration of [18F]FDG uptake and histopathology in surgically excised malignancies of the head and neck: a feasibility study. Eur J Nucl Med Mol Imaging 2023;50(7):2127–39. https://doi.org/10.1007/s00259-023-06153-z.
[23] Rufini V, Garganese G, Ieria FP, Pasciuto T, Fragomeni SM, Gui B, et al. Diagnostic performance of preoperative [18F]FDG-PET/CT for lymph node staging in vulvar cancer: a large single-centre study. Eur J Nucl Med Mol Imaging 2021;48(10):3303–14. https://doi.org/10.1007/s00259-021-05257-8.
[24] Boellaard R, Delgado-Bolton R, Oyen WJG, Giammarile F, Tatsch K, Eschner W, et al. FDG PET/CT: EANM procedure guidelines for tumour imaging: version 2.0. Eur J Nucl Med Mol Imaging 2015;42(2):328–54. https://doi.org/10.1007/s00259-014-2961-x.
[25] Miller TR, Grigsby PW. Measurement of tumor volume by PET to evaluate prognosis in patients with advanced cervical cancer treated by radiation therapy. Int J Radiat Oncol Biol Phys 2002;53:353–9. https://doi.org/10.1016/S0360-3016(02)02705-0.
[26] Kitajima K, Suenaga Y, Ueno Y, Maeda T, Ebina Y, Yamada H, et al. Preoperative risk stratification using metabolic parameters of 18F-FDG PET/CT in patients with endometrial cancer. Eur J Nucl Med Mol Imaging 2015;42(8):1268–75. https://doi.org/10.1007/s00259-015-3037-2.
[27] Quak E, Le Roux P-Y, Hofman MS, Robin P, Bourhis D, Callahan J, et al. Harmonizing FDG PET quantification while maintaining optimal lesion detection: prospective multicentre validation in 517 oncology patients. Eur J Nucl Med Mol Imaging 2015;42(13):2072–82. https://doi.org/10.1007/s00259-015-3128-0.
[28] Mattoli MV, Calcagni ML, Taralli S, Indovina L, Spottiswoode BS, Giordano A. How often do we fail to classify the treatment response with [18F]FDG PET/CT acquired on different scanners? Data from clinical oncological practice using an automatic tool for SUV harmonization. Mol Imag Biol 2019;21:1210–9. https://doi.org/10.1007/s11307-019-01342-5.
[29] Collamati F, van Oosterom MN, De Simoni M, Faccini R, Fischetti M, Mancini Terracciano C, et al. A DROP-IN beta probe for robot-assisted 68Ga-PSMA radioguided surgery: first ex vivo technology evaluation using prostate cancer specimens. EJNMMI Res 2020;10(1). https://doi.org/10.1186/s13550-020-00682-6.
[30] Allison J, Amako K, Apostolakis J, Arce P, Asai M, Aso T, et al. Recent developments in Geant4. Nucl Instrum Methods Phys Res A 2016;835:186–225. https://doi.org/10.1016/j.nima.2016.06.125.
[31] Collamati F, Maccora D, Alfieri S, Bocci V, Cartoni A, Collarino A, et al. Radioguided surgery with β− radiation in pancreatic Neuroendocrine Tumors: a feasibility study. Sci Rep 2020;10(1). https://doi.org/10.1038/s41598-020-61075-2.
[32] Russomando A, Schiariti M, Bocci V, Colandrea M, Collamati F, Cremonesi M, et al. The β- radio-guided surgery: method to estimate the minimum injectable activity from ex-vivo test. Phys Med 2019;58:114–20. https://doi.org/10.1016/j.ejmp.2019.02.004.
[33] Bertani E, Collamati F, Colandrea M, Faccini R, Fazio N, Ferrari ME, et al. First ex vivo results of β-radioguided surgery in small intestine neuroendocrine tumors with 90Y-DOTATOC. Cancer Biother Radiopharm 2021;36(5):397–406. https://doi.org/10.1089/cbr.2020.4487.
[34] Morganti S, Bertani E, Bocci V, Colandrea M, Collamati F, Cremonesi M, et al. Tumor-non-tumor discrimination by a β- detector for Radio Guided Surgery on ex-vivo neuroendocrine tumors samples. Phys Med 2020;72:96–102. https://doi.org/10.1016/j.ejmp.2020.03.021.
[35] Angelone M, Battistoni G, Bellini F, Bocci V, Collamati F, De Lucia E, et al. Properties of para-terphenyl as detector for alpha, beta and gamma radiation. IEEE Trans Nucl Sci 2014;61:1483–7. https://doi.org/10.1109/TNS.2014.2322106.
[36] Collamati F, Moretti R, Alunni-Solestizi L, Bocci V, Cartoni A, Collarino A, et al. Characterisation of a β detector on positron emitters for medical applications. Phys Med 2019;67:85–90. https://doi.org/10.1016/j.ejmp.2019.10.025.
[37] Mirabelli R, Morganti S, Cartoni A, Simoni MD, Faccini R, Fischetti M, et al. Characterization and optimization of a β detector for 18F radio-guided surgery. Phys Med 2023;108. https://doi.org/10.1016/j.ejmp.2023.102545.
[38] El Lakis M, Gianakou A, Nockel P, Wiseman D, Tirosh A, Quezado MA, et al. Radioguided surgery with gallium 68 dotatate for patients with neuroendocrine tumors. JAMA Surg 2019;154(1):40.
[39] Boellaard R. Standards for PET image acquisition and quantitative data analysis. J Nucl Med 2009;50(Suppl 1):11S–20S. https://doi.org/10.2967/jnumed.108.057182.
[40] Bonzom S, Menard L, Pitre S, Duval MA, Siebert R, Palfi S, et al. An intraoperative beta probe dedicated to glioma surgery: design and feasibility study. IEEE T Nucl Sci 2007;54(1):30–41. https://doi.org/10.1109/TNS.2006.885574.